HHS Public Access

Author manuscript

Cell Calcium. Author manuscript; available in PMC 2020 May 06.

Published in final edited form as:

Cell Calcium. 2020 May ; 87: 102187. doi:10.1016/j.ceca.2020.102187.

TRPM7 activation potentiates SOCE in enamel cells but requires ORAI

Guilherme H. Souza Bomfim[a], **Veronica Costiniti**[a], **Yi Li**[a], **Youssef Idaghdour**[b], **Rodrigo S. Lacruz**[a,*]

[a]Department of Basic Science and Craniofacial Biology, New York University College of Dentistry, New York, NY 10010, USA.

[b]Biology Program, Division of Science and Mathematics, New York University Abu Dhabi, Abu Dhabi, United Arab Emirates.

Abstract

Calcium (Ca^{2+}) release-activated Ca^{2+} (CRAC) channels mediated by STIM1/2 and ORAI (ORAI1–3) proteins form the dominant store-operated Ca^{2+} entry (SOCE) pathway in a variety of cells. Among these, the enamel-forming cells known as ameloblasts rely on CRAC channel function to enable Ca^{2+} influx, which is important for enamel mineralization. This key role of the CRAC channel is supported by human mutations and animal models lacking *STIM1* and *ORAI1*, which results in enamel defects and hypomineralization. A number of recent reports have highlighted the role of the chanzyme TRPM7 (transient receptor potential melastanin 7), a transmembrane protein containing an ion channel permeable to divalent cations (Mg^{2+}, Ca^{2+}), as a modulator of SOCE. This raises the question as to whether TRPM7 should be considered an alternative route for Ca^{2+} influx, or if TRPM7 modifies CRAC channel activity in enamel cells. To address these questions, we monitored Ca^{2+} influx mediated by SOCE using the pharmacological TRPM7 activator naltriben and the inhibitor NS8593 in rat primary enamel cells and in the murine ameloblast cell line LS8 cells stimulated with thapsigargin. We also measured Ca^{2+} dynamics in ORAI1/2-deficient (sh*Orai1/2*) LS8 cells and in cells with siRNA knock-down of *Trpm7*. We found that primary enamel cells stimulated with theTRPM7 activator potentiated Ca^{2+} influx via SOCE compared to control cells. However, blockade of TRPM7 with NS8593 did not decrease the SOCE peak. Furthermore, activation of TRPM7 in sh*Orai1/2* LS8 cells lacking SOCE failed to elicit Ca^{2+} influx, and *Trpm7* knock-down had no effect on SOCE. Taken together, our data suggest that TRPM7 is a positive modulator of SOCE potentiating Ca^{2+} influx in enamel cells, but its function is fully dependent on the prior activation of the ORAI channels.

Graphical Abstract

*Corresponding author: Rodrigo S. Lacruz; Department of Basic Science and Craniofacial Biology, New York University College of Dentistry, New York, NY 10010, USA. rodrigo.lacruz@nyu.edu; rsl10@nyu.edu.

Declaration of interest: None

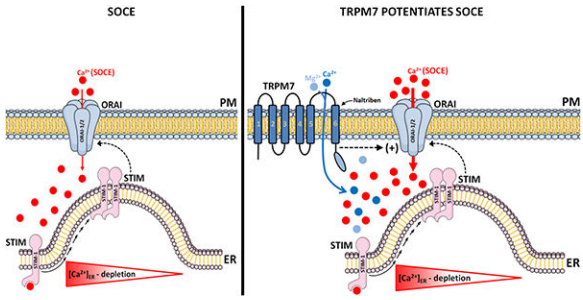

Keywords

Ca^{2+} signaling; CRAC channels; SOCE; TRPM7 channels; enamel cells

1. Introduction

It is well established that calcium (Ca^{2+}) handling is one of the most widespread transducing systems, regulating a wide range of cell biology and pathophysiologic processes [1–5]. Enamel is the most calcified vertebrate tissue, requiring a steady supply of Ca^{2+} for its mineralization. Specialized epithelial cells known as ameloblasts first form, and then mineralize the enamel crystals, supported by adjacent cells of the enamel organ [6]. Enamel development is commonly defined in two stages: 1) a developmental (secretory); and 2) a mineralization (maturation) stage. The latter has been shown to feature a marked increase in ion transport, particularly Ca^{2+}, as crystals grow in thickness [7–9]. Recent studies have shown that a key Ca^{2+} influx pathway in enamel cells is via store-operated Ca^{2+} entry (SOCE) mediated by the Ca^{2+} release-activated Ca^{2+} (CRAC) channels [10–13]. SOCE is widely expressed in many non-excitable cells [14–16]. Physiologically, a depletion in endoplasmic reticulum (ER) Ca^{2+} concentration ($[Ca^{2+}]_{ER}$) triggers the oligomerization and redistribution of the ER resident Ca^{2+} sensors stromal interaction molecules-STIM1 and STIM2 in close proximity to the plasma membrane. At these sites, STIM proteins couple to the highly Ca^{2+}-selective conductance pore known as ORAI proteins (*ORAI1–3*), thereby opening the channel and enabling sustained Ca^{2+} influx [14,17,18].

Pharmacological and molecular data support the crucial role of SOCE in enamel cells. Selective ORAI inhibitors (synta-66, BTP2, GSK7975A) markedly reduce or nearly abolish SOCE in enamel cells, while mutations in *STIM1* or *ORAI1* genes in patients result in abnormal enamel with hypomineralization [7,11]. Mice lacking STIM1/2 or ORAI1 showed deficient SOCE and enamel defects [12,13]. Combined, these data highlight the critical role of SOCE as a key Ca^{2+} influx channel in enamel cells. However, recent reports have revealed that the transient receptor potential melastanin 7 (TRPM7) is a modulator of SOCE [19,20] and that *Trpm7*-inactive knock-in mutant mice exhibited hypomineralized enamel [21]. As the genetic disruption of TRPM7 ($Trpm7^{-/-}$) is embryonic lethal in mice [21,22], analyses of the enamel phenotype performed in heterozygous mice showed deficient mineralization of their enamel and cranial bones [21]. These phenotypes were attributed to Mg^{2+} deficiency, which was required for alkaline phosphatase activity and mineralization [21]. In addition to reduced enamel volume, another study suggested that TRPM7 was

involved in the early stages of amelogenesis via cAMP response element binding protein (CREB) [23]. Therefore, both TRPM7 and CRAC components are expressed in enamel cells, and it would be of interest to understand the potential functional links between these two distinct channels.

The ORAI family of proteins (ORAI1–3) bear little homology to other channels and are quite distinct from TRPM7 [16]. All ORAI proteins share a structure with both N- and C-termini located in the cytosol and display four transmembrane (TM) domains with two extra and two intracellular loops [14,16]. ORAI proteins likely form heteromeric units and it is generally considered that hexamers of the first TM of ORAI1 form the central pore [16], lined by a number of glutamate amino acids near the outer end that confer high Ca^{2+} selectivity [16,24]. TRPM7 is an ubiquitous transmembrane protein composed of an ion channel permeable to divalent cations (Mn^{2+}, Ca^{2+}, Mg^{2+}, Co^{2+}, Ni^{2+} and Zi^{2+}) fused to a C-terminal α-kinase domain that phosphorylates downstream substrates [25,26]. TRPM7 contains six TM domains, with the channel pore found between TM5 and TM6 and the kinase domain in the C-terminus [27]. Ion channels exist in multiple highly dynamic conformational states associated with transitions between open, closed and inactivated steady-state [27–29]. A recent report showed lower cell proliferation in TRPM7 kinase-dead (KD) K1646R knock-in mice associated with inactivated (non-conducting state) or loss of pre-activated state of TRPM7 in K1646R knock-in mice [20].

Some of the main physiological functions of TRPM7 channels include maintaining the intracellular level of Mg^{2+} linked with cell proliferation and differentiation, regulating cell volume and playing a role in the immune system [22,30]. Recent evidence also indicates that TRPM7 not only contributes to Ca^{2+} homeostasis [19, 25, 31], but is also found in intracellular vesicles distinct from those of the endocytotic pathway [32]. Although several molecular targets have been postulated, the cellular and functional mechanisms through which TRPM7 activation occurs remain unclear [31]. TRPM7 have been linked to different downstream signaling pathways through the C-terminal α-kinase domain [25]. Previous evidence reported that the TRPM7 channel is activated by agonists of G protein-coupled receptors (GPCR) coupled to phospholipase C (PLC) [25,31]. From a pharmacologic viewpoint, a number of TRPM7 modulators, such as the selective agonist gating-modulator of the TRPM7 channel naltriben [33] and the reversible Mg^{2+}-dependent TRPM7 channels antagonist NS8593, [34] allow us to tease apart the function of TRMP7 in enamel cells *in vitro* [33–35].

Given the important role of SOCE in enamel formation [10–12], and that TRPM7 is able to conduct Ca^{2+} as well [25], this raises the issue of whether TRPM7 can directly act as a Ca^{2+} influx channel or a modulator of SOCE in enamel cells. This will have implications for developing models of Ca^{2+} homeostasis in enamel cells and, potentially, for developing enamel regeneration models, as these depend on a full understanding of the physiological requirements of ameloblasts to induce mineralization. Using rat primary enamel cells from the secretory and maturation stages and the ameloblast cell line LS8 cells, we show that activation of the TRPM7 channel enhances Ca^{2+} influx, but only after SOCE stimulation. Moreover, TRPM7 activation cannot elicit Ca^{2+} influx in ORAI1/ORAI2-deficient ameloblasts and *Trpm7* knock-down has no effect on Ca^{2+} influx via SOCE. Taken together,

our findings suggest that TRPM7 is unable to stimulate Ca^{2+} influx in enamel cells in the absence of ORAI proteins. It can, however, positively modulate the effects of SOCE following CRAC channel activation.

2. Materials and methods

2.1 Animal use

All procedures employed in this study were conducted in accordance with guidelines approved by the Institutional Animal Care and Use Committee (IACUC) of New York University College of Dentistry (protocol # IA16–00625).

2.2 Primary cell culture and line

Male and female Sprague Dawley rats (100–120 g) were used to isolate secretory (SEC) and maturation (MAT) enamel organ (EO) cells from the lower incisors, as previously described [9,12,36]. To obtain single cell populations, isolated cell clumps from each stage were transferred to Eppendorf tubes containing 1mL of Hanks' balanced salt solution (Thermo Fisher, USA; #:14065-056) with 1% Antibiotic-Antimycotic (Thermo Fisher, USA; #:15240-062). Subsequently, EO cells were digested with 0.25 mg/ml of Liberase TL (Roche, Germany; #414654) for 30 minutes at 37°C in a 5%-CO_2 incubator, manually pipetted every 10 minutes to mechanically separate the cells. The enzymatic reaction was stopped by adding 2mL of X-Vivo™ 15 (Lonza Bioscince, USA; #: 04–418Q) cell media containing 10% FBS (Thermo Fisher, USA; #:12483-020) and 1% Penicillin-Streptomycin (Thermo Fisher, USA; #:15140-122). Cells were centrifuged at 500 X g for 5 minutes, washed twice and plated on glass cover slips coated with Corning™ Cell-Tak (Fisher Scientific, USA; #:CB-40240). To confirm the isolation of SEC and MAT cell populations, we measured the mRNA expression of enamelin (ENAM) and ameloblast-associated protein (ODAM) that are the major secreted products of secretory and maturation stage ameloblasts, respectively [7,9, Fig. S1, A and B]. Isolated SEC and MAT cells were used within 24 hours after dissection. To increase cell purity in primary EO cells, we labeled fibroblasts using a PE-conjugated monoclonal anti-rat CD90 antibody. The immortalized murine ameloblasts cell line LS8 cells [37] that have been used widely to study various aspects of enamel development [38] were also used. LS8 cells are a good model to study Ca^{2+} signaling in the context of enamel formation as they express functional SOCE and the molecular components of the CRAC channels [10,12].

2.3 Retroviral transduction and siRNA

shRNAs against *Orai1*, *Orai2* or *Renilla* (as a negative control) were cloned into the shRNA scaffold of the pLMP-mirE11 retroviral backbone (expressing GFP and puromycin resistance), as recently described [12]. To generate siRNA against *Trpm7*, LS8 cells were seeded at a density of 1.10^6 cells/well in 6-well plates and grown in DMEM (Thermo Fisher, USA; #:11885-092) containing 10% FBS and antibiotics. One day after seeding, cells (60–80% confluent) were transfected with siRNA against mouse *Trpm7* using ON-TARGETplus Mouse Trpm7 reagents (Dharmacon, USA; #:J-040716-06-0002), according to the manufacturer's instructions. Briefly, the plasmid containing *Trpm7* siRNA (6 μL) was diluted in DMEM (150 μL) and transfected with Lipofectamine™ RNAiMAX (Termo

Fisher, USA; #:13778-075) at a 1:1 ratio. After mixing at room temperature, the *Trpm7* siRNA-lipid complex (25 pM) was incubated drop-wise onto the cells and cultured for two days. Control cells were exposed to transfectant in the absence of siRNA using ON-TARGETplus Non-targeting Pool (Dharmacon, USA; #:D-001810-10-05). Transfection and knock-down efficiency were monitored at the mRNA levels by RT-PCR of *Trpm7* expression.

2.4 Real-time PCR of *Orai1*, *Orai2* and *Trpm7*

Total RNA was isolated using the RNeasy Micro Kit (Qiagen, USA; #:74004), as indicated by the manufacturer, followed by reverse transcription using the iScript™ cDNA Synthesis Kit (Bio-Rad, USA; #:1708890). For qRT-PCR, we used the SsoAdvanced™ Universal SYBR® Green Supermix (Bio-Rad, USA; #:1725270) and performed the experiments in a CFX Connect thermocycler (Bio-Rad, USA). *Gapdh* and *β-actin* were used as housekeeping genes. All primers were used at 0.25 nM. Relative quantification of gene expression was determined by the $2^{-\Delta\Delta CT}$ method [11,12]. All primer sequences used are shown in Table S1.

2.5 $[Ca^{2+}]_{cyt}$ measurements

Cytosolic Ca^{2+} concentration ($[Ca^{2+}]_{cyt}$) measurements of SEC and MAT and LS8 cells were performed as described [10–12]. Briefly, cells were incubated for one hour at room temperature with 1 μM of a ratiometric Ca^{2+} probe, Fura-2-AM (Thermo Fisher, USA; #:F-1221), in Ca^{2+}-free Ringer's solution (pH 7.4) composed as follows (mM): 155.0 NaCl; 4.5 KCl; 1.0 $MgCl_2$; 10 D-glucose; and 10 HEPES (Sigma-Aldrich, USA). To increase cell purity in primary EO cells, we labeled fibroblasts using a PE-conjugated monoclonal anti-rat CD90 antibody (1:500 dilution) (BioLegend, USA; #:105201) and excluded the latter from further analysis, as previously described [11]. Fluorescence recordings were obtained by: 1) an inverted light microscope (Nikon 2000U Eclipse, Japan) equipped with an objective (Nikon S Fluor × 20; numerical aperture: 0.45) coupled to device camera (CoolSNAP HQ_2 CCD Camera; Photometrics, USA), controlled by computer software (NIS Elements version 4.20.01, USA); or 2) an inverted light microscope (Nikon Ti2-E Eclipse, Japan) equipped with an objective (Nikon S Fluor × 20; numerical aperture: 0.75) and a digital SLR camera (DS-Qi2; Nikon, Japan) controlled by computer software (NIS Elements version 5.20.01, USA).

Cells were continuously perfused by a six- or eight-way perfusion system (VC-6/8 valve controller) at 5–6 ml per minute with a common outlet 0.28-mm tube driven by electrically controlled valves (Harvard Bioscience Inc., USA). A normal Ringer's solution (the same Ca^{2+}-free Ringer's solution, however, containing 2mM of Ca^{2+}) or a Ca^{2+}-free solution were used to dissolve all drugs (at room temperature). Fura-2-AM was excited alternatively at 340 and 380 nm using a Lambda LS xenon-arc lamp (Sutter Instrument, USA) or pE-340 fura (Cool Led, USA). Emitted fluorescence was collected through a 510 nm emission filter. Fluorescence images were generated at 5-second intervals and the ratio values were calculated. A Fura-2 calcium imaging calibration kit (Thermo Fisher, USA; #:F6774) was used to estimate the $[Ca^{2+}]_{cyt}$, according to the manufacturer's specifications. Standard control buffer (background fluorescence), zero free-Ca^{2+} buffer (free-Ca^{2+}) and 39 μM free-

Ca^{2+} buffer (saturating Ca^{2+}) were used to convert the emission ratio at 340/380 nm excitation to estimate the free $[Ca^{2+}]_{cyt}$.

2.5.1 SOCE measurements—To measure SOCE, ER Ca^{2+} store depletion was stimulated by pre-incubation with 1 μM of thapsigargin (Sigma-Aldrich, USA; #:T9033) for 20 minutes prior to the experimental protocols in Ca^{2+}-free Ringer's solution. Subsequently, under fluorescence recordings, cells were continuously perfused for 120 seconds with Ca^{2+}-free Ringer's solution, followed by a re-addition of 2 mM of extracellular Ca^{2+} in normal Ringer's solution to measure the delta (Δ) SOCE peak. To block SOCE, cells were also preincubated with pharmacological CRAC antagonists synta-66 (5 μM) (Sigma-Aldrich, USA; #:1949) or with 3,5-bis trifluoromethyl pyrazole-BTP-2 (20 μM) (Sigma-Aldrich, USA; #:203890) for two hours [10,14,39]. Synta-66 concentration was determined after the construction of the concentration-effect curve (Fig. S2, B). The TRPM7 agonist, naltriben (NAL, 100 μM) (Tocris Bioscience, USA; #:0892) [31,35], was perfused simultaneously with the Ca^{2+} re-addition for 720 seconds. In other sets of experiments, the TRPM7 antagonist NS8593 (30 μM) (Tocris Bioscience, USA; #:4597) was simultaneously perfused during the Ca^{2+} re-addition, in the absence or presence of naltriben (100 μM), as described [35].

2.6 Bioinformatic analyses

The Pfam protein families database release, 32.0 [40], was used to retrieve information about the various domains of *TRPM7* (UniProt ID Q923J1). Release 32.0 improved refinement of domain boundaries and their functional annotation. In particular, we highlight two domains in the TRPM7 protein: 1) the ion transfer domain of 246 amino acids (855–1108 amino acid equivalent to alignment region 858–1104 aa in Q923J1) spanning over exons 19–24 (this domain has six transmembrane helices in which the last two helices flank a loop that determines ion selectivity); 2) the MHCK/EF2 kinase domain of 195 amino acids (1617–1814 amino acid equivalent to alignment region 1619–1814 aa in Q923J1) spanning over exons 34–38 of isoform Trpm7–202. The kinase domain is from the alpha-kinase family [41]. Ensembl genome browser 97 was used to visualize the gene and the localization of the domains identified by Pfam release 32.0 as well as other databases (Fig. S5).

2.7 Data analyses and statistics

All data, mathematical analyses and graphs were analyzed and/or generated using the GraphPad Prism software version 8.0 (Inc., California, USA). The Δ SOCE peak, SOCE slope and area under the curve (A.U.C.) were calculated by integrating the transients versus time during the stimulus duration for each experiment. The SOCE slope (increase or decrease) parameter was fitted by the GraphPad Prism software using the one-phase association equation [2]. Data represents the mean ± SEM of the minimum of three independent experiments. Differences between the means of the group data that fit a normal distribution were analyzed using a two-tailed unpaired Student's t-test variance or, when indicated, a one-way ANOVA followed by a Bonferroni's multiple comparison post-hoc test. The limit of significance was established at $^{*}P < 0.05$; $^{**}P < 0.01$; $^{***}P < 0.001$; $^{\#}P < 0.05$ vs. SEC group; n.s., non-significant.

3. Results

3.1 TRPM7 activation enhances SOCE in enamel cells

To determine the maximum capacity of Ca^{2+} mobilization of the well-known pharmacological TRPM7 activator, naltriben [33,34], we first constructed concentration-effect curves in LS8 cells as a reference (Fig. 1, A–B). The ameloblasts LS8 cells have been widely used in enamel research and also show robust SOCE [10,12,38]. Naltriben peaks were shown at 100 μM, as also reported elsewhere [35,42]. We used this concentration in primary cells and analyzed the effects of naltriben (NAL,100 μM) in secretory and maturation -stage ameloblasts under resting levels (2 mM Ca^{2+}) showing that naltriben elicited a very small elevation in Ca^{2+} influx (~16 nM) in cells of both stages (Fig. 1, C–D). In addition, we found a small increase (~12 nM) in cytosolic Ca^{2+} in naltriben-stimulated cells in Ca^{2+}-free solution (Fig. 1, E–F), suggesting that TRPM7 channels might release Ca^{2+} from the ER.

To address whether TRPM7 is involved in Ca^{2+} influx mediated by SOCE in enamel cells, we first measured the expression level of *Orai1* and *Trpm7* by RT-PCR. Both *Orai1* and *Trpm7* expression levels were higher (~95% and ~65%, respectively) in maturation cells (Fig. 2, A–B). We also analyzed SOCE in primary enamel cells from the secretory and maturation stages without TRPM7 activation. All cells were pre-treated with thapsigargin (1 μ M, 20 minutes) to passively and maximally deplete the ER Ca^{2+} stores before measuring SOCE by re-addition of 2 mM Ca^{2+}. Fura-2-AM-loaded cells showed significantly higher SOCE in maturation (Fig. 2, C–F). These data are also consistent with the increased expression and function of both STIM1 and ORAI1 in maturation stage by RT-PCR and protein level as we have reported elsewhere [10].

When perfused simultaneously during Ca^{2+} re-addition, naltriben (100 μM) was able to enhance SOCE in both secretory and maturation stage cells (Fig. 2 C–F). The delta (Δ) peak of Ca^{2+} influx was ~3-fold and ~2-fold higher in secretory and maturation, respectively, when TRPM7 was activated. The speed of Ca^{2+} influx also increased (Fig. 2 E). Taken together, these functional data indicate that the pharmacological activation of TRPM7 channel activity potentiates SOCE in primary enamel cells of both stages, although the enhancing effects are higher in secretory cells despite elevated levels of *Trpm7* expression in maturation.

This difference between gene expression levels and potentiation of Ca^{2+} influx is unclear, but could be linked to the buffering capacity of SOCE by mitochondria [43], as mitochondria are more abundant in maturation stage cells [44] and therefore could sequester a higher Ca^{2+} load. Alternatively, Broertjes et al., [45] showed that overexpression of TRPM7 increases Ca^{2+} influx when associated with upregulation of second messengers (PKC and PKA). We also analyzed the possible effects of naltriben (100 μM) in $[Ca^{2+}]_{cyt}$ clearance (Fig. S3 A). Our data showed a decrease (~45%) in the slope of SOCE inactivation only in secretory stage cells (Fig. S3 C), suggesting faster inactivation kinetics of Ca^{2+} transients after naltriben stimulation.

3.2 Effects of ORAI and TRPM7 blockade in Ca^{2+} influx

We then compared the effects of blocking ORAI channels and TRPM7 using pharmacological inhibitors. First, we depleted the Ca^{2+} stores with thapsigargin to stimulate SOCE in the presence and absence of the ORAI blockers synta-66 or BTP-2. Both inhibitors decreased Ca^{2+} influx significantly, showing lower Ca^{2+} peaks in secretory and maturation stage cells (Fig. 3, A–B and E–F) as well as other parameters (Fig. 3, C–D and G–H).

To assess whether TRPM7 contributes to SOCE or if TRPM7 is a positive modulator of SOCE, we measured Ca^{2+} influx in primary enamel cells after depleting the Ca^{2+} stores with thapsigargin to stimulate SOCE in the presence of the TRPM7 channel inhibitor NS8693. Delta SOCE peak, SOCE slope and A.U.C. parameters did not show a reduction in maturation stage cells when exposed to NS8693 (30 μM) (Fig. 4, A–D). However, NS8593-(30 μM) treated secretory cells showed an increase (~35%) in Ca^{2+} influx (Fig. 4, A–D). A plausible explanation for this could be related to the structural similarities between NS8593 with a benzimidazole homologue (NNC 55–0396), which may interact with a common ligand-binding site in TRPM7 with distinct functional consequences for channel function, as previously suggested [33–35]. Since TRPM7 blockade did not decrease SOCE, these data suggest that the TRPM7 channel is not a component of SOCE in enamel cells.

We next addressed the question of whether potentiating TRPM7 in the presence of NS8593 (30 μM) modified the kinetics of Ca^{2+} influx. Primary enamel cells were simultaneously stimulated with naltriben (100 μM) and the antagonist NS8693 (30 μM), and were compared to cells stimulated only with naltriben. The combined treatment of naltriben and NS8693 showed a significant decrease in both secretory and maturation stage cells in the Δ peak (~53% and ~45%), slope (~37% and ~35%) and A.U.C. (~44% and ~49%) (Fig. 4, E–H). This suggests that NS8593 can inhibit a portion of Ca^{2+} influx in SOCE that is mediated by TRPM7. Combined, these data indicate that pharmacological blockade of TRPM7 does not decrease SOCE in enamel cells, but ORAI inhibition does. Furthermore, TRPM7 is not required for SOCE. This suggests that TRPM7 is not a component of SOCE in enamel cells, but can function as a positive modulator when activated, thereby enhancing SOCE. In addition, the SOCE enhancement mediated by TRPM7 activation can be reversed by blocking the channel with NS8593.

3.3 siRNA knock-down of TRPM7 has no effect on SOCE

We next generated a *Trpm7* knock-down in the murine enamel cell line LS8 cells (si*Trpm7*) to test its effects on SOCE using a siRNA vector containing three strands (see Methods). Bioinformatics analyses revealed that two of these siRNA strands targeted the channel and the kinase domains of TRPM7 (Fig. S5). A knock-down of *Trpm7* expression was confirmed by RT-PCR analysis, showing a dramatic decrease in mRNA of ~90% (Fig. 5, A). In si*Trpm7* cells (*Trpm7* KD), *Orai1* and *Orai2* expression was unchanged (Fig. 5, B–C). In addition, we tested the effects of naltriben (100 μM) during Ca^{2+} influx via SOCE in *Trpm7* KD cells. As expected, control LS8 cells (non-targeting pool) stimulated with naltriben (100 μM) during Ca^{2+} re-addition revealed a potentiation in SOCE, represented by increased Δ Ca^{2+} influx peak (~70%), SOCE slope rate (~32%) and A.U.C (~40%) parameters (Fig. 5, D–G), confirming that TRPM7 positively modulates SOCE in this cell type. Despite

significantly decreased TRPM7 expression in si*Trpm7* cells, SOCE was unchanged compared to controls, even after stimulating these cells with naltriben (100 μM) (Fig. 5, D–G). These data support a non-essential role of TRPM7 in SOCE in enamel cells.

3.4 TRPM7 potentiation is dependent on the prior activation of ORAI

To more directly address possible links between ORAI proteins and TRPM7 in mediating Ca^{2+} influx in enamel cells, we used our previously developed ORAI1/ORAI2-deficient (sh*Orai1/2*) LS8 cells [12] to measure Ca^{2+} influx following SOCE stimulation in the presence of naltriben. As predicted, RT-PCR analysis revealed decreased expression of *Orai1* (~66%) and *Orai2* (~75%), and in LS8 cells of sh*Orai1/2* (Fig. 6, A–B). Interestingly, *Trpm7* expression was also significantly decreased (~42%) in sh*Orai1/2* cells (Fig. 6, C). sh*Orai1/2* LS8 cells were shown to have minimally residual SOCE (Fig. 6, E–G), possibly mediated by ORAI3, as discussed elsewhere [12]. Importantly, we show that sh*Orai1/2* LS8 cells stimulated with naltriben (100 μM) during the Ca^{2+} re-addition failed to elicit a raise in $[Ca^{2+}]_{cyt}$ mediated by SOCE (Fig. 6, D). The Δ Ca^{2+} influx peak SOCE slope rate and A.U.C. remained unchanged (Fig. 6, E–G).These results suggest an essential role of ORAI proteins in Ca^{2+} influx. They also indicate the potentiation of SOCE by TRPM7 activation is dependent on ORAI proteins.

4. Discussion

Ca^{2+} is an essential component of mineralized enamel. Transepithelial Ca^{2+} transport by ameloblasts requires Ca^{2+} uptake prior to its delivery to the extracellular space. In enamel cells, the bulk of Ca^{2+} influx is mediated by SOCE [6,10,46]. The chanzyme TRPM7 has been recently described as being a SOCE modulator [19], while other studies show abnormal enamel in *Trpm7*-deficient mice [20], raising the possibility that TRPM7 may act as a modulator of Ca^{2+} influx in enamel cells. Here, we show that pharmacological activation of TRPM7 in enamel cells positively enhances SOCE (Fig. 1, C–F), thereby participating in Ca^{2+} influx. These effects, however, depend on the prior activation of SOCE. In TRPM7-deficient enamel cells, SOCE was unaffected (Fig. 5, D–G), suggesting that TRPM7 is a positive modulator but non-essential for SOCE.

Besetty et al., [20] showed that inactivation of the kinase domain of TRPM7 results in reduced SOCE in T cells of TRPM7 kinase-dead mice. Specifically, Faouzi and colleagues suggested that the downregulation of SOCE in *Trpm7*-deficient chicken B-lymphocytes was mediated by the phosphorylation of STIM2 by the kinase domain of TRPM7 [19]. In our study of enamel cells, we have addressed two main questions using Ca^{2+} imaging data: 1) is the TRPM7 channel a component of SOCE; and 2) can TRPM7 modulate SOCE?

Using rat enamel organs to isolate ameloblasts from secretory and maturation stage [46], we show that both cells have SOCE, with significantly higher Ca^{2+} influx in maturation (Fig. 2, C–F), in keeping with our previous findings [10,11]. To ascertain if TRPM7 affected Ca^{2+} influx following SOCE activation, secretory and maturation cells were perfused with the TRPM7 agonist naltriben, which elicited an increase of the SOCE signal (Fig 2, C–F). Naltriben is a selective gating modulator of the TRPM7 channel insensitive to intracellular Mg^{2+} levels [35]. It is also known as a delta (Δ) opioid receptor antagonist. A previous

mRNA screen did not identify the expression of this opioid receptor in enamel cells [47]. These findings implicate TRPM7 as a novel physiological channel functionally involved in Ca^{2+} handling in enamel cells.

To confirm that the enhancement of SOCE mediated by naltriben was associated with TRPM7, we used the TRPM7 channel blocker NS8593. This compound is a potent TRPM7 channel inhibitor [48] and Faouzi et al., showed that NS8593 significantly inhibited SOCE in rat basophilic leukemia cells when used at the same concentration as in our study (30 μM) [19]. It is also known to block Ca^{2+} responses in mouse eggs during fertilization [49]. In enamel cells, however, NS8593 did not inhibit SOCE. Rather, it inhibited only the TRPM7-induced enhancement of SOCE mediated by the agonist naltriben (Fig. 4, E–H). These data confirm that naltriben activate the TRPM7 channel to participate in Ca^{2+} influx. By contrast, primary enamel cells treated with the CRAC channel blockers BTP-2 and synta-66 significantly reduced Ca^{2+} influx by SOCE (Fig. 3, A–H). These pharmacological approaches indicate that inhibition of TRPM7 does not affect SOCE in enamel cells, but blockade of ORAI channels significantly diminishes Ca^{2+} influx, confirming that SOCE is the main mediator of Ca^{2+} uptake. These results highlight that the TRPM7 channel is a positive modulator of Ca^{2+} influx via SOCE in enamel cells, but not a component of SOCE. This conclusion is in agreement with the Faouzi et al., results in DT40 chicken cells [19].

The efficiency of the TRPM7 channel in Ca^{2+} influx in enamel cells was further investigated using a molecular approach. Using our previously [12] developed enamel cell line LS8 cells lacking *Orai1* and *Orai2* (sh*Orai1/2*), we first tested the expression of *Trpm7* in these cells by RT-PCR. The expression of *Trpm7* was downregulated in sh*Orai1/2* cells (Fig. 6, C), suggesting a molecular link between these two proteins (see also below). However, naltriben stimulation of TRPM7 in sh*Orai1/2* cells, which show nearly abolished Ca^{2+} influx, failed to elicit a raise in Ca^{2+} uptake. This was not the case in control LS8 cells where, similar to primary cells, naltriben enhanced SOCE (Fig. 6, D–G). The inability of the TRPM7 channel agonist to elevate cytosolic Ca^{2+} in sh*Orai1/2* cells indicates that the channel function of TRPM7 is dependent on previous activation of the ORAI pore. Given that *Trpm7* expression was significantly decreased in sh*Orai1/2* cells, however, the possibility that TRPM7 could not be effectively activated in sh*Orai1/2* cells remained unclear.

To address this, we generated a knock-down of *TRPM7* by siRNA in LS8 cells (si*Trpm7*). The double-stranded RNA molecules in the vector used here contained a mixture of four siRNA as a single reagent, including strands that targeted the channel and kinase regions of *TRPM7* (see methods and Fig. S5). The expression of *Trpm7* was dramatically decreased in si*Trpm7* LS8 cells, but *Orai1* or *Orai2* expression was unchanged (Fig 5, A–C). As noted above, disrupting *Orai1/Orai2* results in a decrease of *Trpm7* expression, but the opposite does not appear to have a bearing on *Orai1/Orai2* expression. This might indicate a dependence of TRPM7 expression on ORAI, but not the opposite. This scenario requires further analysis that is beyond the scope of the present study. Despite the significant reduction of *Trpm7* expression in si*Trpm7* LS8 cells, however, our data clearly show that SOCE was unaffected (Fig 5, A–G). This contrasts with data on splenocytes of TRPM7 kinase-dead K1646R knock-in mice, in which SOCE was significantly reduced [20]. However, the TRPM7 agonist, naltriben (100 μM), showed a decrease in A.U.C. in TRPM7

KD cells (Fig. 5 G), indicating a reduction in the total Ca^{2+} mobilization due a faster inactivation kinetics after stimulation. Similarly, Inoue et al., [50] showed that naltriben (50 μM) increases a TRPM7-like current and $[Ca^{2+}]_{cyt}$ in adipocytes, that they associated with changes in Ca^{2+} clearance. This suggests that naltriben (50–100 μM) may affect clearance mechanisms (PMCAs or Na^{+}/Ca^{2+} exchangers).

The possibility that TRPM7 is found in intracellular vesicles of enamel cells and the potential of these vesicles to contribute to changes in cytosolic Ca^{2+} were not directly addressed here. However, the small of changes in cytosolic Ca^{2+} in naltriben-stimulated cells in Ca^{2+}-free solution (Fig. 1, E–F) suggests that, if these TRPM7-expressing vesicles are to be found in enamel cells, their contribution to Ca^{2+} signaling is minor. The possibility that naltriben is inefficient in activating intracellular TRPM7 channels cannot be discounted.

In summary, this study used pharmacological and molecular approaches to investigate the role of the TRPM7 channel on SOCE in enamel cells. We showed that the TRPM7 Ca^{2+}-permeable channel itself is not a SOCE component. We also show that the enhancement of SOCE potentiated by TRPM7 activation depends on the previous activation of ORAI. These data indicate an indirect, but positive potentiating role of the TRPM7 channel on SOCE in enamel cells.

Supplementary Material

Refer to Web version on PubMed Central for supplementary material.

Acknowledgements

This work was supported by the National Institute of Dental and Craniofacial Research (NIDCR) (grants DE027679 and DE025639) to RSL. YI is funded by New York University Abu Dhabi research grant AD105. Computational analysis is supported by CGSB Core Bioinformatics resources. We are thankful to Dr. Bimal Desai for discussions and two anonymous reviewers for their comments that helped improve the manuscript.

References

[1]. Lacruz RS, Feske S, Diseases caused by mutations in ORAI1 and STIM1. Ann. N. Y. Acad. Sci 1356, 45–79 (2015). DOI: 10.1111/nyas.12938. [PubMed: 26469693]

[2]. Souza Bomfim GH, Mendez-Lopez I, Arranz-Tagarro JA, et al., Functional Upregulation of STIM-1/Orai-1-Mediated Store-Operated Ca2+ Contributing to the Hypertension Development Elicited by Chronic EtOH Consumption. Curr Vasc Pharmacol. 2017;15(3):265–281. DOI: 10.2174/1570161115666170201122750. [PubMed: 28155613]

[3]. Berridge MJ, Lipp P, Bootman MD, The versatility and universality of calcium signalling. Nat Rev Mol Cell Biol. 2000 10;1(1):11–21. DOI: 10.1038/35036035. [PubMed: 11413485]

[4]. Carafoli E, Calcium signaling: a tale for all seasons. Proc Natl Acad Sci U S A. 2002 2 5;99(3):1115–22. DOI: 10.1073/pnas.032427999. [PubMed: 11830654]

[5]. Clapham DE, Calcium signaling. Cell. 2007 12 14;131(6):1047–58. DOI: 10.1016/j.cell.2007.11.028. [PubMed: 18083096]

[6]. Lacruz RS, Enamel: Molecular identity of its transepithelial ion transport system. Cell Calcium 65, 1–7 (2017). DOI: 10.1016/j.ceca.2017.03.006. [PubMed: 28389033]

[7]. Eckstein M, Aulestia FJ, Nurbaeva MK, Lacruz RS, Altered Ca2+ signaling in enamelopathies. Biochim. Biophys. Acta 1865, 1778–1785 (2018). DOI: 10.1016/j.bbamcr.2018.04.013.

[8]. Smith CE, Cellular and chemical events during enamel maturation. Crit Rev Oral Biol Med. 1998;9(2):128–61. DOI: 10.1177/10454411980090020101. [PubMed: 9603233]

[9]. Lacruz RS, Smith CE, Bringas PJ, et al., Identification of novel candidate genes involved in mineralization of dental enamel by genome-wide transcript profiling. J. Cell. Physiol 227, 2264–2275. DOI: 10.1002/jcp.22965.

[10]. Nurbaeva MK, Eckstein M, Concepcion AR, et al., Dental enamel cells express functional SOCE channels. Sci. Rep 5, 15803 (2015). DOI: 10.1038/srep15803. [PubMed: 26515404]

[11]. Nurbaeva MK, Eckstein M, Devotta A, et al., Evidence That Calcium Entry Into Calcium-Transporting Dental Enamel Cells Is Regulated by Cholecystokinin, Acetylcholine and ATP. Front Physiol. 2018 Jul 2;9:801 DOI: 10.3389/fphys.2018.00801.

[12]. Eckstein M, Vaeth M, Aulestia FJ, et al., Differential regulation of Ca2+ influx by ORAI channels mediates enamel mineralization. Sci Signal. 2019 4 23;12(578). pii: eaav4663. DOI: 10.1126/scisignal.aav4663.

[13]. Eckstein M, Vaeth M, Fornai C, et al., Store-operated Ca2+ entry controls ameloblast cell function and enamel development. JCI Insight. 2017 3 23;2(6):e91166 DOI: 10.1172/jci.insight.91166. [PubMed: 28352661]

[14]. Putney JW, Forms and functions of store-operated calcium entry mediators, STIM and Orai. Adv Biol Regul. 2018 5;68:88–96. DOI: 10.1016/j.jbior.2017.11.006. [PubMed: 29217255]

[15]. Parekh AB, Store-operated CRAC channels: function in health and disease. Nat Rev Drug Discov. 2010 5;9(5):399–410. DOI: 10.1038/nrd3136. [PubMed: 20395953]

[16]. Prakriya M, Lewis RS, Store-Operated Calcium Channels. Physiol Rev. 2015 10;95(4):1383–436. DOI: 10.1152/physrev.00020.2014. [PubMed: 26400989]

[17]. Zhang SL, Yu Y, Roos J, et al., STIM1 is a Ca2+ sensor that activates CRAC channels and migrates from the Ca2+ store to the plasma membrane. Nature. 2005 10 6;437(7060):902–5. DOI: 10.1038/nature04147. [PubMed: 16208375]

[18]. Smyth JT, Hwang SY, Tomita T, DeHaven WI, Mercer JC, Putney JW, Activation and regulation of store-operated calcium entry. J Cell Mol Med. 2010 10;14(10):2337–49. DOI: 10.1111/j.1582-4934.2010.01168.x. [PubMed: 20807283]

[19]. Faouzi M, Kilch T, Horgen FD, Fleig A, Penner R, The TRPM7 channel kinase regulates store-operated calcium entry. J Physiol. 2017 5 15; 595(10): 3165–3180. DOI: 10.1113/JP274006. [PubMed: 28130783]

[20]. Beesetty P, Wieczerzak KB, Gibson JN, et al., Inactivation of TRPM7 kinase in mice results in enlarged spleens, reduced T-cell proliferation and diminished store-operated calcium entry. Sci Rep. 2018; 8: 3023 DOI: 10.1038/s41598-018-21004-w. [PubMed: 29445164]

[21]. Nakano Y, Le MH, Abduweli D, et al., A Critical Role of TRPM7 As an Ion Channel Protein in Mediating the Mineralization of the Craniofacial Hard Tissues. Front Physiol. 2016 7 6;7:258 DOI: 10.3389/fphys.2016.00258. [PubMed: 27458382]

[22]. Ryazanova LV, Rondon LJ, Zierler S, et al., TRPM7 is essential for Mg2+ homeostasis in mammals. Nat Commun. 2010 11 2; 1: 109 DOI: 10.1038/ncomms1108. [PubMed: 21045827]

[23]. Ogata K, Tsumuraya T, Oka K, et al., The crucial role of the TRPM7 kinase domain in the early stage of amelogenesis. Sci Rep. 2017; 7: 18099 DOI: 10.1038/s41598-017-18291-0. [PubMed: 29273814]

[24]. Fahrner M, Schindl R, Romanin C, Studies of Structure-Function and Subunit Composition of Orai/STIM Channel Calcium Entry Channels in Non-Excitable Cells. Boca Raton (FL): CRC Press/Taylor & Francis; 2018 Chapter 2.

[25]. Zou Z, Rios FJ, Montezano AC, Touyz RM, TRPM7, Magnesium, and Signaling. Int J Mol Sci. 2019 4; 20(8): 1877 DOI: 10.3390/ijms20081877.

[26]. Cohen RM, Moiseenkova-Bell VY, Structure of Thermally Activated TRP Channels. Curr Top Membr. 2014; 74: 181–211. DOI: 10.1016/B978-0-12-800181-3.00007-5. [PubMed: 25366237]

[27]. Nadler MJ, Hermosura MC, Inabe K, et al., LTRPC7 is a Mg.ATP-regulated divalent cation channel required for cell viability. Nature. 2001 5 31;411(6837):590–5. DOI: 10.1038/35079092. [PubMed: 11385574]

[28]. Lau C, Hunter MJ, Stewart A, Perozo E, Vandenberg JI, Never at rest: insights into the conformational dynamics of ion channels from cryo-electron microscopy. J Physiol. 2018 4 1; 596(7): 1107–1119. DOI: 10.1113/JP274888. [PubMed: 29377132]

[29]. Minor DL, Let It Go and Open Up, an Ensemble of Ion Channel Active States. Cell. 2016 2 11;164(4):597–8. DOI: 10.1016/j.cell.2016.01.037. [PubMed: 26871624]

[30]. Sahni J, Tamura R, Sweet IR, Scharenberg AM, TRPM7 regulates quiescent/proliferative metabolic transitions in lymphocytes. Cell Cycle. 2010 9 1; 9(17): 3565–3574. DOI: 10.4161/cc.9.17.12798. [PubMed: 20724843]

[31]. Chubanov V, Mittermeier L, Gudermann T, Role of kinase-coupled TRP channels in mineral homeostasis. Pharmacol Ther. 2018 4;184:159–176. DOI: 10.1016/j.pharmthera.2017.11.003. [PubMed: 29129644]

[32]. Abiria SA, Krapivinsky G, Sah R, et al., TRPM7 senses oxidative stress to release Zn2+ from unique intracellular vesicles. Proc Natl Acad Sci U S A. 2017 7 25; 114(30): E6079–E6088. DOI: 10.1073/pnas.1707380114. [PubMed: 28696294]

[33]. Chubanov V, Ferioli S, Gudermann T, Assessment of TRPM7 functions by drug-like small molecules. Cell Calcium. 2017 11;67:166–173. DOI: 10.1016/j.ceca.2017.03.004. [PubMed: 28356194]

[34]. Chubanov V, Schäfer S, Ferioli S, Gudermann T, Natural and Synthetic Modulators of the TRPM7 Channel. Cells. 2014 12; 3(4): 1089–1101. DOI: 10.3390/cells3041089. [PubMed: 25437439]

[35]. Schäfer S, Ferioli S, Hofmann T, Zierler S, Gudermann T, Chubanov V, Mibefradil represents a new class of benzimidazole TRPM7 channel agonists. Pflugers Arch. 2016 4;468(4):623–34. DOI: 10.1007/s00424-015-1772-7. [PubMed: 26669310]

[36]. Smith CE, Nanci A, A method for sampling the stages of amelogenesis on mandibular rat incisors using the molars as a reference for dissection. Anat Rec. 1989 11;225(3):257–66. DOI: 10.1002/ar.1092250312. [PubMed: 2683870]

[37]. Chen LS, Couwenhoven RI, Hsu D, Luo W, Snead ML, Maintenance of amelogenin gene expression by transformed epithelial cells of mouse enamel organ. Arch. Oral Biol 37, 771–778 (1992). DOI: 10.1016/0003-9969(92)90110-T. [PubMed: 1444889]

[38]. Sarkar J, Simanian EJ, Tuggy SY, et al., Comparison of two mouse ameloblast-like cell lines for enamel-specific gene expression. Front. Physiol 5, 277 (2014). DOI: 10.3389/fphys.2014.00277. [PubMed: 25120490]

[39]. Zitt C, Strauss B, Schwarz EC, et al., Potent inhibition of Ca2+ release-activated Ca2+ channels and T-lymphocyte activation by the pyrazole derivative BTP2. J Biol Chem. 2004 3 26;279(13):12427–37. DOI: 10.1074/jbc.M309297200. [PubMed: 14718545]

[40]. El-Gebali S, Mistry J, Bateman A, et al., The Pfam protein families database in 2019. Nucleic Acids Res. 2019 1 8;47(D1):D427–D432. DOI: 10.1093/nar/gky995. [PubMed: 30357350]

[41]. Ryazanov AG, Pavur KS, Dorovkov MV MV, Alpha-kinases: a new class of protein kinases with a novel catalytic domain. Curr Biol. 1999 1 28;9(2):R43–5. DOI: 10.1016/s0960-9822(99)80006-2.

[42]. Hofmann T, Schäfer S, Linseisen M, Sytik L, Gudermann T, Chubanov V, Activation of TRPM7 channels by small molecules under physiological conditions. Pflugers Arch. 2014 12;466(12):2177–89. DOI: 10.1007/s00424-014-1488-0. [PubMed: 24633576]

[43]. Malli R, Graier WF, The Role of Mitochondria in the Activation/Maintenance of SOCE: The Contribution of Mitochondrial Ca2+ Uptake, Mitochondrial Motility, and Location to Store-Operated Ca2+ Entry. Adv Exp Med Biol. 2017;993:297–319. DOI: 10.1007/978-3-319-57732-6_16. [PubMed: 28900921]

[44]. Ohshima H, Maeda T, Takano Y, Cytochrome oxidase activity in the enamel organ during amelogenesis in rat incisors. Anat Rec. 1998 12;252(4):519–31. DOI: 10.1002/(SICI)1097-0185(199812)252:4<519::AID-AR3>3.0.CO;2-I. [PubMed: 9845203]

[45]. Broertjes J, Klarenbeek J, Habani Y, Langeslag M, Jalink K, TRPM7 residue S1269 mediates cAMP dependence of Ca2+ influx. PLoS One. 2019; 14(1): e0209563 DOI: 10.1371/journal.pone.0209563. [PubMed: 30615643]

[46]. Lacruz RS, Habelitz S, Wright JT, Paine ML ML, Dental Enamel Formation and Implications for Oral Health and Disease. Physiol Rev. 2017 7 1;97(3):939–993. DOI: 10.1152/physrev.00030.2016. [PubMed: 28468833]

[47]. Won J, Vang H, Kim JH, Lee PR, Kang Y, Oh SB, TRPM7 Mediates Mechanosensitivity in Adult Rat Odontoblasts. J Dent Res. 2018 8;97(9):1039–1046. DOI: 10.1177/0022034518759947. [PubMed: 29489440]

[48]. Chubanov V, y Schnitzler MM, Meißner M, Schäfer S, Abstiens K, Hofmann T, Gudermann T, Natural and synthetic modulators of SK (Kca2) potassium channels inhibit magnesium-dependent activity of the kinase-coupled cation channel TRPM7. Br J Pharmacol. 2012 6; 166(4): 1357–1376. DOI: 10.1111/j.1476-5381.2012.01855.x. [PubMed: 22242975]

[49]. Bernhardt ML, Padilla-Banks E, Stein P, Zhang Y, Williams CJ, Store-operated Ca2+ entry is not required for fertilization-induced Ca2+ signaling in mouse eggs. Cell Calcium. 2017 7;65:63–72. DOI: 10.1016/j.ceca.2017.02.004. [PubMed: 28222911]

[50]. Inoue H, Inazu M, Konishi M, Yokoyama U, Functional expression of TRPM7 as a Ca2+ influx pathway in adipocytes. Physiol Rep. 2019 10; 7(20): e14272 DOI: 10.14814/phy2.14272. [PubMed: 31650715]

Highlights

- SOCE mediated by CRAC channels is enhanced upon activation of TRPM7 in enamel cells
- TRPM7 blockade or TRPM7 knock-down does not affect SOCE in enamel cells
- Stimulation of TRPM7 in ORAI1/2-deficient enamel cells failed to elevate $[Ca^{2+}]i$
- TRPM7 is not essential for SOCE but can enhance it

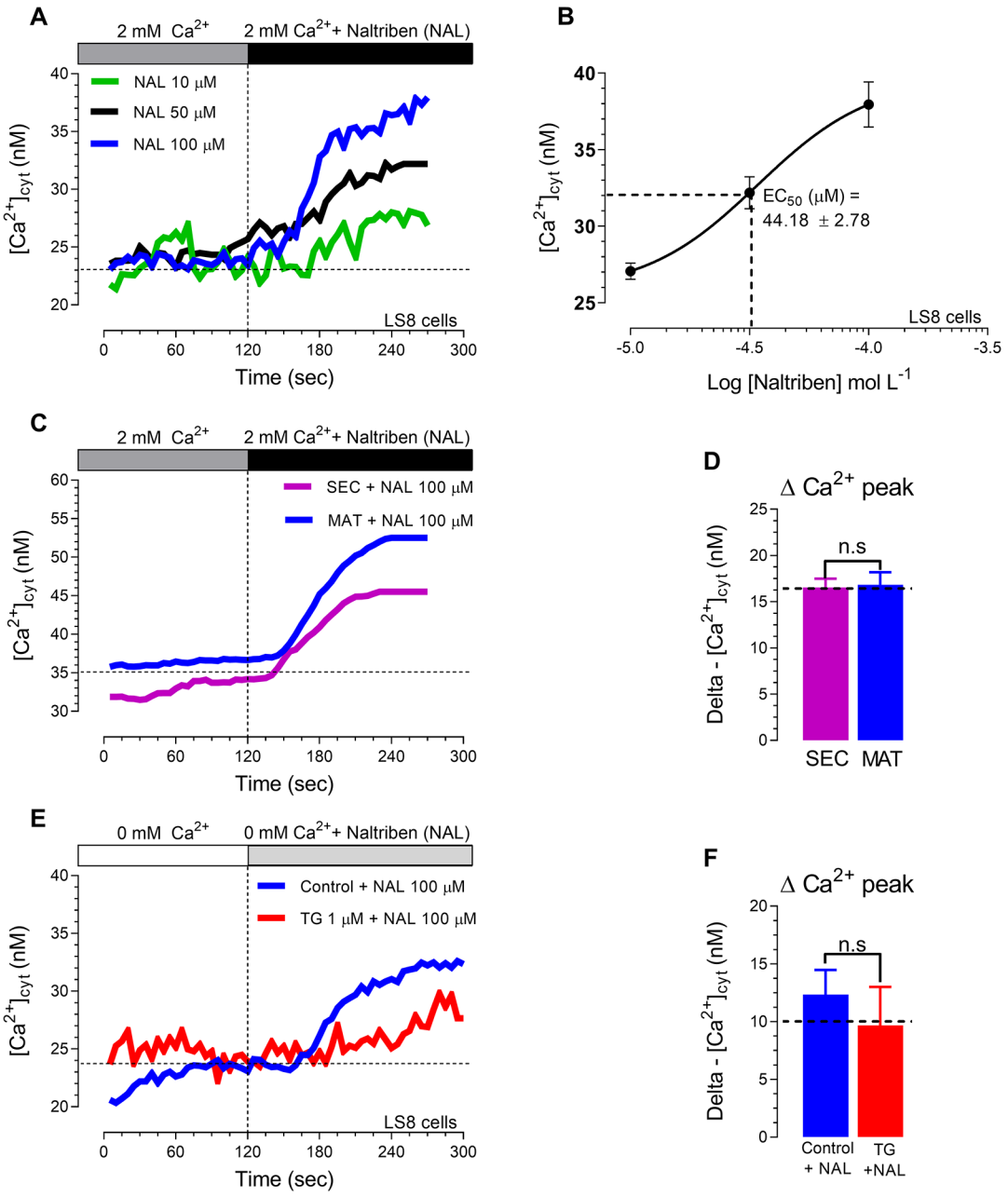

Figure 1. Effects of the TRPM7 activator, naltriben (NAL), in ameloblast cell line LS8 and primary enamel cells.

We constructed a concentration-effect curve in the enamel cell line (LS8 cells) using the well-known pharmacological TRPM7 activator, naltriben **(A-B)**, to determine the maximum capacity of Ca^{2+} mobilization. Naltriben showed an EC_{50} around 45 μM **(B)** with Ca^{2+} peak in LS8 cells at 100 μM **(A-B)**. We then used naltriben (100 μM) in primary ameloblasts from the secretory (SEC) and maturation (MAT) stages, **(C-D)**. Changes in $[Ca^{2+}]_{cyt}$ transients were monitored using naltriben (100 μM) after ER-Ca^{2+} depletion with thapsigargin (1 μM, 20 min, red trace) or without store depletion (blue trace) **(E-F)**. Data represent the mean ±

SEM of minimum three independent experiments. Data analyzed by two-tailed unpaired Student's t-test at $*P < 0.05$; $**P < 0.01$; $***P < 0.001$; n.s., non-significant.

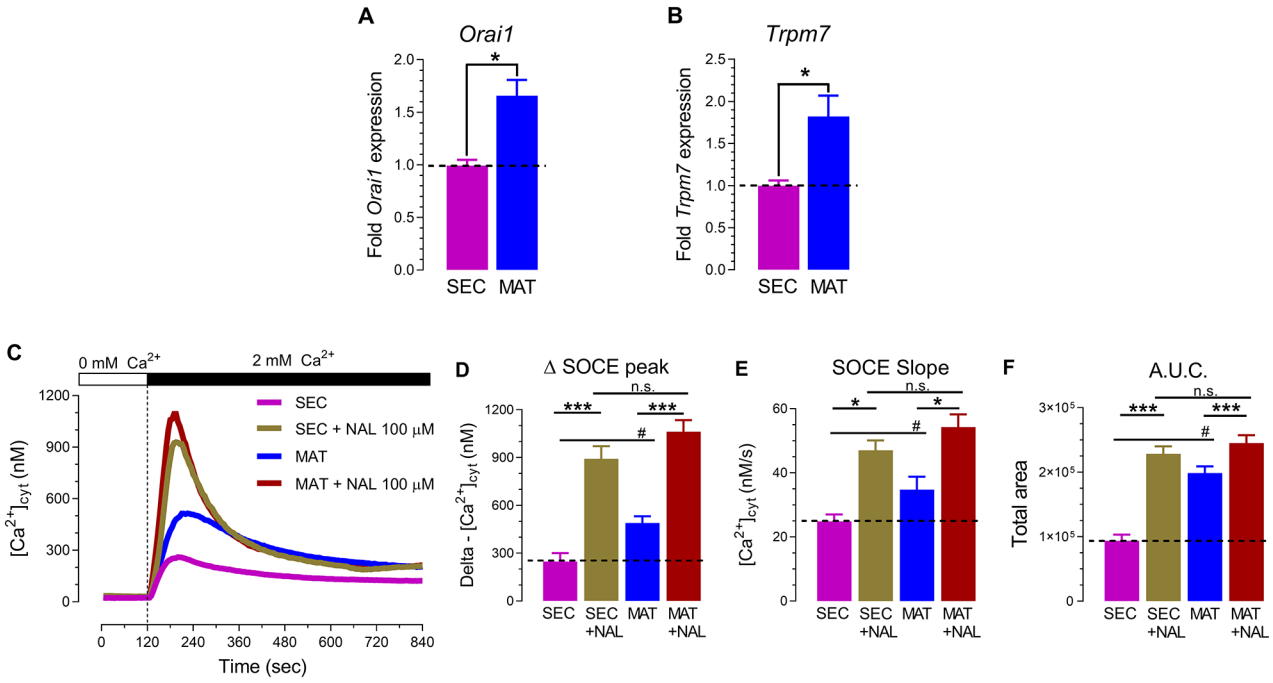

Figure 2. TRPM7 channel activation potentiates Ca^{2+} influx via SOCE in primary enamel cells.

RT-PCR analyses of secretory (SEC) and maturation (MAT) stage enamel organ cells show increased expression of *Orai1* **(A)** and *Trpm7* **(B)** in maturation. **(C)** Representative original traces of $[Ca^{2+}]_{cyt}$ transients in SEC and MAT ameloblasts recorded after pre-incubation with thapsigargin (20 minutes, 1 µM), followed by perfusion with a Ca^{2+}-free Ringer's solution (120 seconds) before simultaneous re-addition of 2 mM extracellular Ca^{2+} and naltriben (NAL,100 µM). **(D)** Quantification of delta SOCE peak, **(E)** SOCE slope, and **(F)** area under the curve (A.U.C.) data represent the mean ± SEM of minimum three independent experiments. Data analyzed by two-tailed unpaired Student's t-test at $^{*}P < 0.05$; $^{**}P < 0.01$; $^{***}P < 0.001$ or one-way ANOVA followed by a Bonferroni's multiple comparison post-hoc test at $^{\#}P < 0.05$ vs. SEC group; n.s., non-significant.

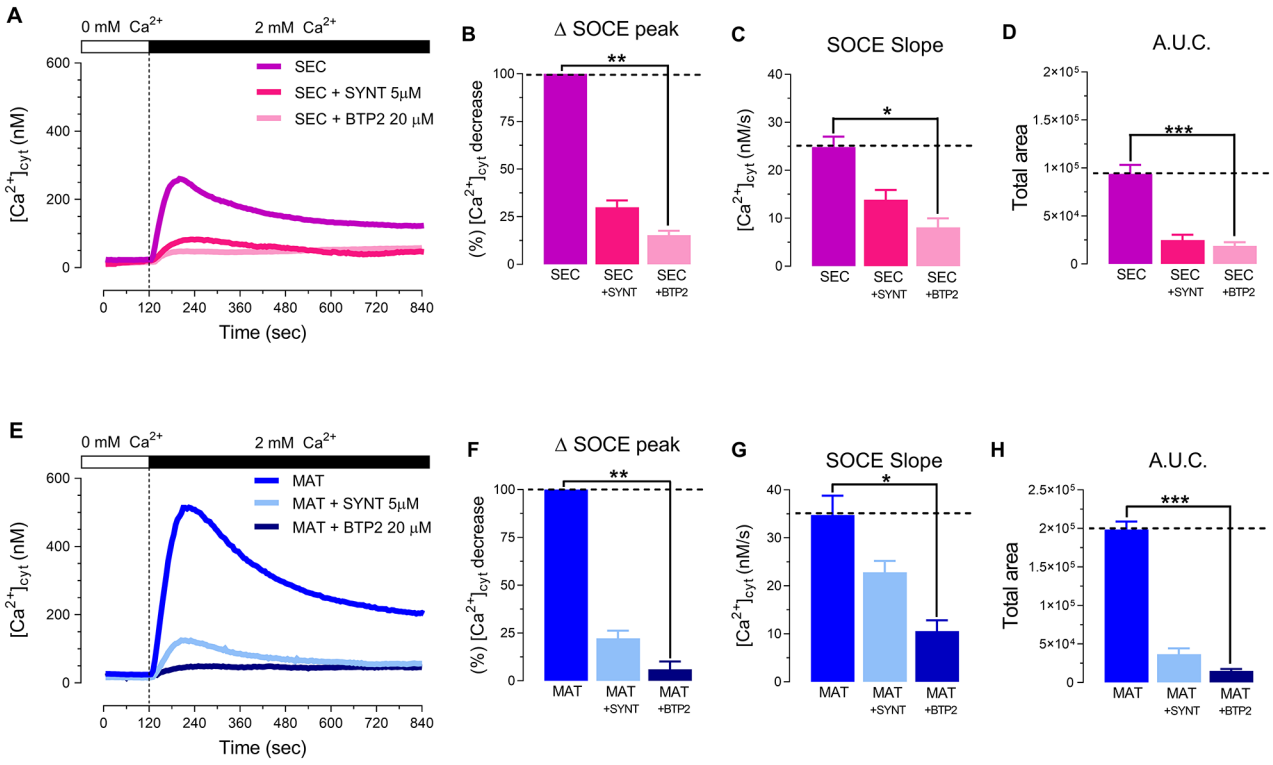

Figure 3. Selective pharmacological inhibition of ORAI in primary enamel cells.

Representative original traces from secretory (SEC) **(A)** and maturation (MAT) **(E)** ameloblasts exposed to the CRAC channel antagonists (synta-66, 5 μM or BTP-2, 20 μM). Both ORAI blockers provoked a substantial reduction in delta SOCE peak **(B, F)**, SOCE slope **(C, G)** and A.U.C. **(D, H)** Data represent the mean ± SEM of minimum three independent experiments. Data analyzed by one-way ANOVA followed by a Bonferroni's multiple comparison post-hoc test at $*P < 0.05$; $**P < 0.01$; $***P < 0.001$.

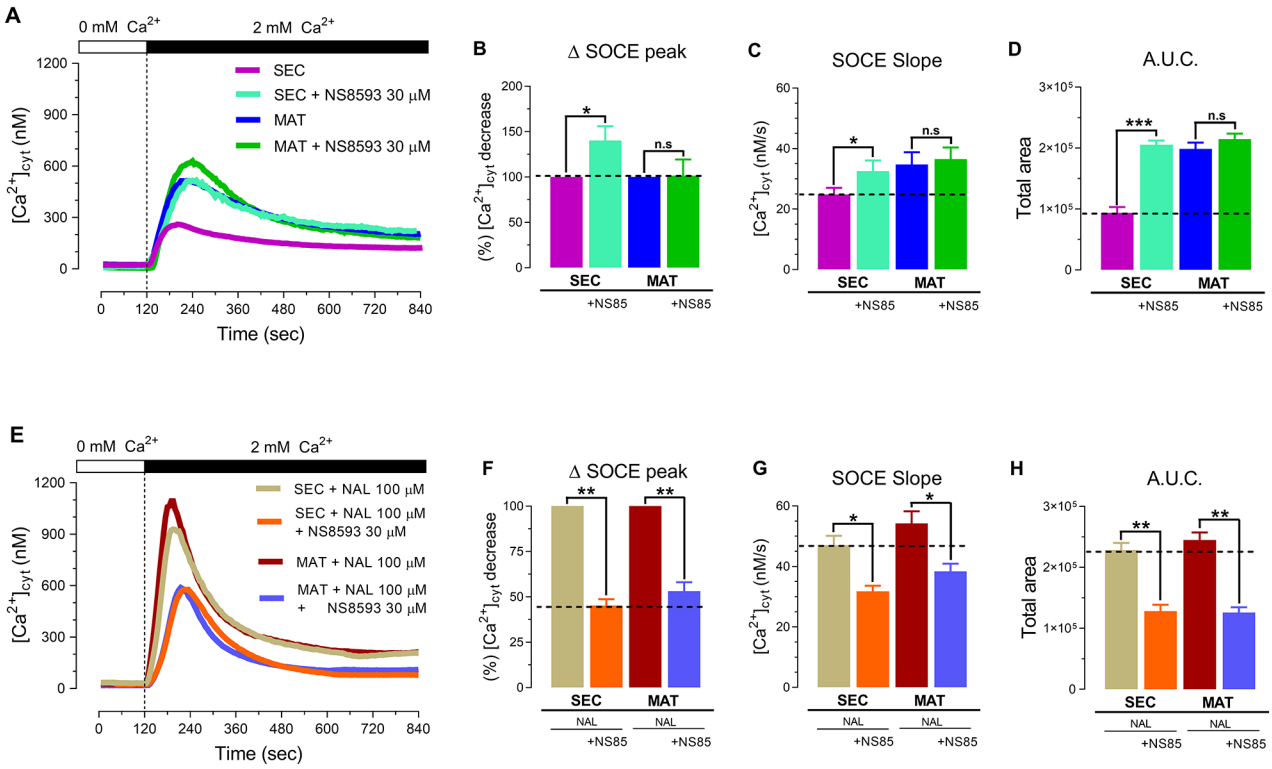

Figure 4. TRPM7 inhibition reverses Ca^{2+} influx potentiation, but does not decrease SOCE in primary enamel cells.

(A) Representative original traces of $[Ca^{2+}]_{cyt}$ transients in control secretory (SEC) and maturation (MAT) stage ameloblasts and in cells exposed to the TRPM7 channel inhibitor NS8693 (30 μM). NS8693 did not elicit a reduction in delta SOCE peak **(B)**, SOCE slope **(C)** or A.U.C. **(D)** in SEC or MAT cells. **(E)** Primary SEC and MAT cells stimulated with naltriben (NAL,100 μM) to active TRPM7 in the presence of NS8593 (30 μM) results in a significant decrease in delta SOCE peak **(F)**, SOCE slope **(G)** and A.U.C. **(H)** Data represent the mean ± SEM of minimum three independent experiments. Data analyzed by two-tailed unpaired Student's t-test at $*P < 0.05$; $**P < 0.01$; $***P < 0.001$; n.s., non-significant.

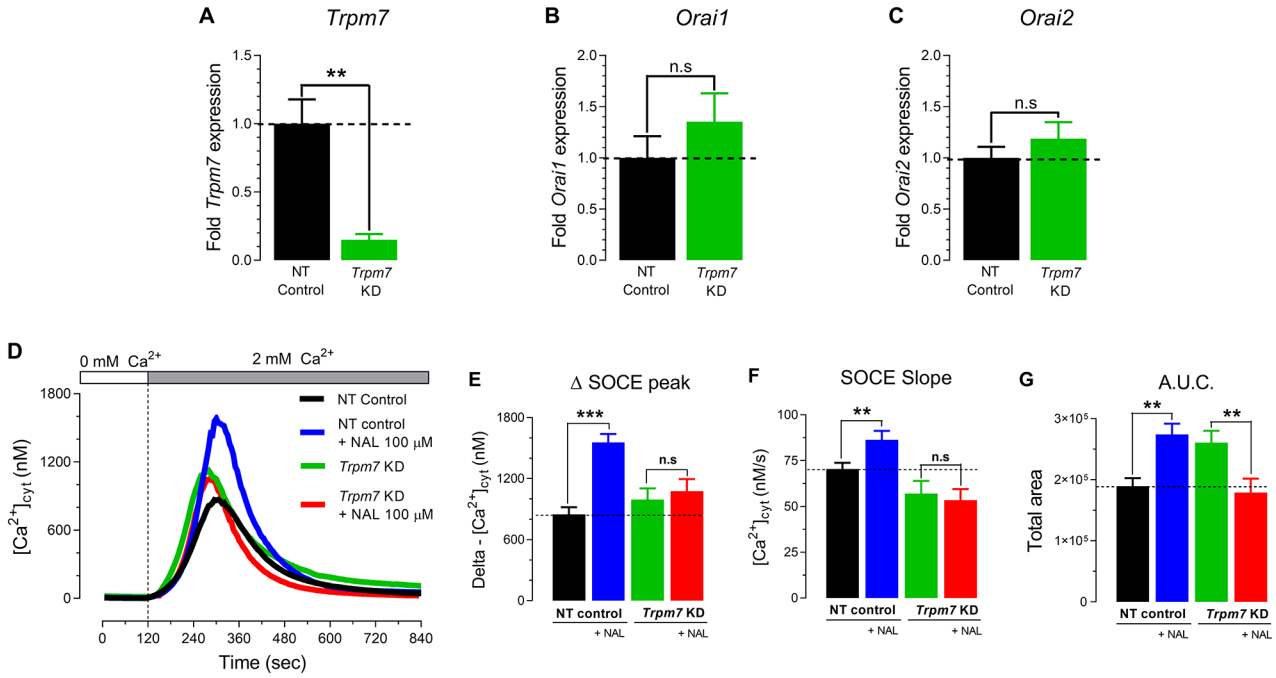

Figure 5. TRPM7 knock-down does not decrease SOCE in the ameloblast cell line LS8 cells.

(A-C) mRNA expression of *Trpm7*, *Orai1* and *Orai2* and in *Trpm7* knock-down (si*Trpm7*) LS8 cells by RT-PCR. **(D)** Representative original tracings of $[Ca^{2+}]_{cyt}$ transients in LS8 cells measured after pre-incubation with thapsigargin (20 minutes, 1 µM), followed by perfusion with a Ca^{2+}-free Ringer's solution (120 seconds) before the simultaneous re-addition of 2 mM extracellular Ca^{2+} to stimulate SOCE in the presence or absence of naltriben (NAL,100 µM). TRPM7 activation elicited by NAL (100 µM) does not potentiate the delta SOCE peak **(E)**, SOCE slope **(F)** or A.U.C. **(G)** in si*Trpm7* LS8 cells. Data represent the mean ± SEM of minimum three independent experiments indicated in the histogram bars. Data analyzed by two-tailed unpaired Student's t-test at $*P < 0.05$; $**P < 0.01$; $***P < 0.001$; n.s., non-significant.

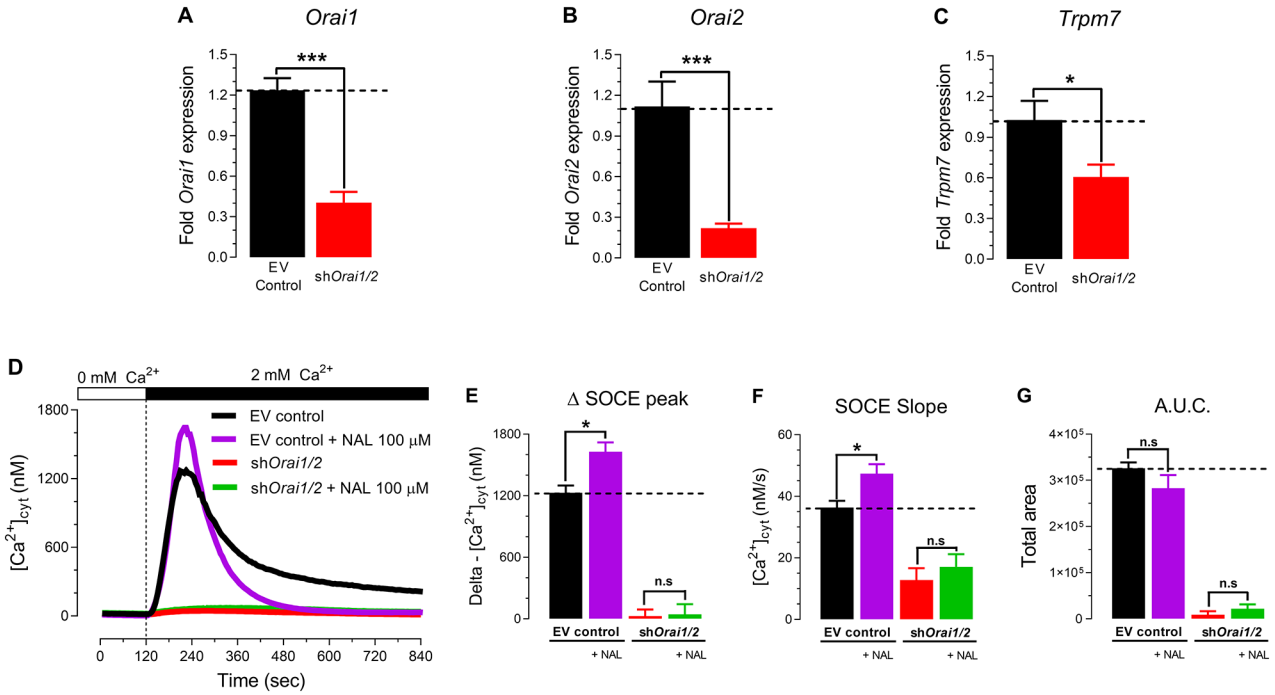

Figure 6. Ca^{2+} influx via the TRPM7 channel depends on ORAI in the ameloblast cell line LS8 cells.

(A-C) Expression of *Orai1*, *Orai2* and *Trpm7* in sh*Orai1/2* LS8 cells, a murine ameloblast cell line, by RT-PCR. **(D)** Representative original traces of $[Ca^{2+}]_{cyt}$ transients in sh*Orai1/2* cells and controls (transfected with empty vector) measured after pre-incubation with thapsigargin (20 minutes, 1 µM), followed by perfusion with a Ca^{2+}-free Ringer's solution (120 seconds) before simultaneous re-addition of 2 mM extracellular Ca^{2+} or with 2 mM Ca^{2+} and naltriben (NAL,100 µM). TRPM7 activation triggered by naltriben (NAL, 100 µM) of sh*Orai1/2* LS8 cells failed to elicit a rise in delta SOCE peak **(E)**, SOCE slope **(F)** or A.U.C. **(G)**. Data represent the mean ± SEM of minimum three independent experiments. Data analyzed by two-tailed unpaired Student's t-test at $*P < 0.05$; $**P < 0.01$; $***P < 0.001$; n.s., non-significant.